Organic LETTERS

Letter

pubs.acs.org/OrgLett

Heteroatom-Bridged Tetraphenylenes: Synthesis, Structures, and Properties

Xiao-Dong Xiong,[†] Chun-Lin Deng,[†] Xiao-Shui Peng,[†,‡] Qian Miao,[†] and Henry N. C. Wong*[,†,‡]

[†]Department of Chemistry, State Key Laboratory of Synthetic Chemistry, Center of Novel Functional Molecules and Institute of Molecular Functional Materials, The Chinese University of Hong Kong, Shatin, New Territories, Hong Kong SAR, China

[‡]Shenzhen Municipal Key Laboratory of Chemical Synthesis of Medicinal Organic Molecules & Shenzhen Center of Novel Functional Molecules, Shenzhen Research Institute, The Chinese University of Hong Kong, No. 10, second Yuexing Road, Shenzhen 518507, China

Supporting Information

ABSTRACT: Novel oxygen-, nitrogen-, sulfur-, and selenium-bridged tetraphenylenes were prepared from known tetraphenylene derivatives. Structures of these compounds were unambiguously confirmed by X-ray crystallographic analyses. Photophysical and electrochemical investigations of these heteroatom-bridged tetraphenylenes suggested their potential applications as electronic materials.

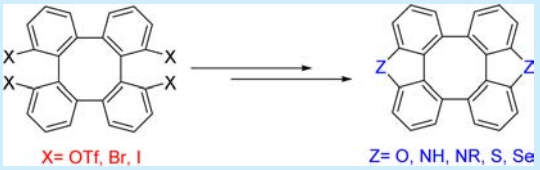

Tetraphenylene (**1**) is unique with a saddle-shaped structure, in which the two opposite pairs of benzene rings are arranged up and down the plane of the eight-membered ring (Figure 1).[1] Various substituted tetraphenylenes with particular rigidity were employed as asymmetric catalysts,[2] liquid crystals,[3] molecular devices,[4] and blue organic light-emitting diodes.[5] The extraordinary geometry of **1** has renewed the interest of several research groups to explore new strategies to install functional groups on tetraphenylenes or to embed tetraphenylenes into conjugated systems.[6] For instance, the annulation of small membered rings and rigid planar π-systems to **1** could planarize its cyclooctatetraene ring. In this domain, Högberg,[7a] Nishinaga,[7b] and Pittelkow[6b,7c] synthesized a class of coplanar antiaromatic cyclooctatetraenes with heteroatom bridges. Herein, we report our own efforts in the synthesis and studies of dioxo, diaza-, dithio-, and diseleno-bridged tetraphenylenes in order to explore the chemistry of these novel heteroatom-bridged tetraphenylenes.

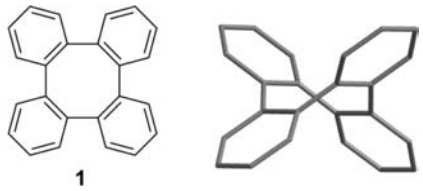

Figure 1. Saddle-shaped structure of tetraphenylene **1**.

Recently, an efficient synthesis of tetraphenylene triflate **2** has been reported.[2a,8] An accidental conversion of **2** to the oxygen-bridged tetraphenylene **3** in the presence of $Pd(PPh_3)_4$ and K_3PO_4 for 24 h at 140 °C in 68% yield was uncovered, as depicted in Scheme 1. Presumably, the tetraphenylene triflate **2** could be partially hydrolyzed into a hydroxyl compound in the presence of a trace amount of water from the commercially available DMF, which then underwent an intramolecular coupling to afford the oxygen-bridged tetraphenylene **3**. Yellowish needle-like single crystals of tetraphenylene **3** were obtained by sublimation of **3** at 295 °C under N_2, whose structure was confirmed by an X-ray crystallographic analysis.

Scheme 1. Synthesis of 3

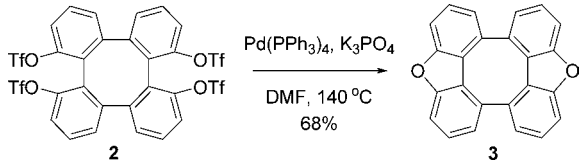

As shown in Scheme 2, upon treatment of 1,8,9,16-tetrabromotetraphenylene (**4**)[9] with sodium azide and CuI/

Scheme 2. Synthesis of 5, 6, and 7

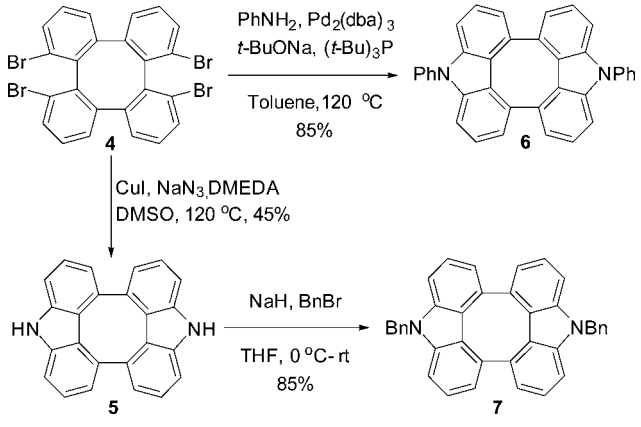

Received: May 3, 2014
Published: June 9, 2014

   dx.doi.org/10.1021/ol501267z | *Org. Lett.* 2014, 16, 3252–3255

N,N′-dimethylethylenediamine (DMEDA) at 120 °C in DMSO, nitrogen-bridged tetraphenylene **5** was obtained in 45% yield. Compound **6** was effectively synthesized via a palladium-mediated double *N*-arylation with aniline at 120 °C in 85% yield. Benzylation of **5** allowed us to produce *N*-benzyl tetraphenylene **7** in 85% yield. Structures of **6** and **7** were unambiguously confirmed by X-ray crystallographic analyses.

With oxygen/nitrogen-bridged tetraphenylenes **3**, **5**, **6**, and **7** in hand, we then turned our attention to the syntheses of sulfur- and selenium-bridged tetraphenylenes **8** and **10**. Although we were unable to convert compound **4** to **8** in a direct manner employing K_2S, treatment of **4** with *n*-BuLi and I_2,[10] followed by a coupling reaction with K_2S in the presence of CuI/DMEDA at 140 °C in CH_3CN, nonetheless provided **8** in 69% yield. Upon treatment of **4** with *n*-BuLi and selenium powder, compound **9** was obtained in 67% yield. Subsequently, a mixture of a copper powder and the solid form of **9** underwent thermal deselenation, leading to the desired **10** in a quantitative yield (Scheme 3). Structures of **8** and **10** were also confirmed by X-ray crystallographic studies.

Scheme 3. Synthesis of 8 and 10

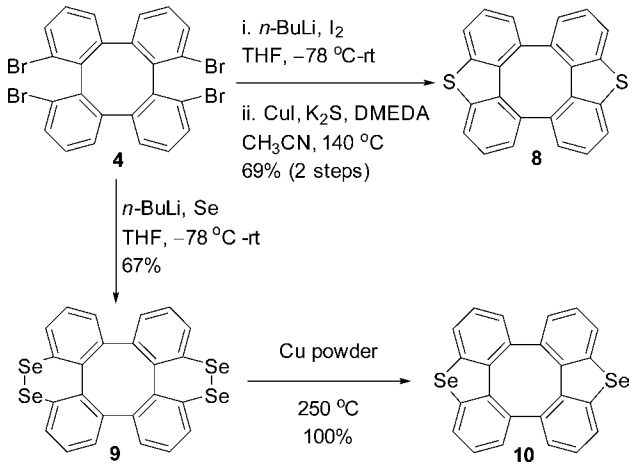

As shown in Table 1, X-ray crystallographic data indicate that these heteroatom-bridged tetraphenylenes (**3**, **6**, **7**, **8**, **10**) are saddle-shaped. As regarding the inner angles of the central eight-membered ring, the average values in the crystal structure of **3**, **7**, **8**, and **10** are found to be 132.2°, 131.1°, 128.7°, and 128.0°, respectively, which are larger than the inner angle of a regular tetraphenylene **1** (122.5°).[2b] However, the average bent angles α of **3**, **7**, **8**, and **10** are 25.6°, 28.8°, 35.3°, and 37.4°, respectively, which are substantially less than that of **1** (50.7°).[2b] Thus, these heteroatom-bridged tetraphenylenes (**3**, **6**, **7**, **8**, **10**) are less puckered than that of **1**, and the heteroatomic bridges effectively force the adjacent two benzene rings to become nearly coplanar, which was further supported by the results of smaller dihedral angles between the pentacyclic and benzene ring (A/B, 7.6°, 14.8°, 12.7°, and 9.4°, respectively). Investigation of the bond lengths in the cyclooctatetraene rings of **3**, **7**, **8**, and **10** reveals that although the average values of the bonds are close to the corresponding values of **1**, the oxygen, nitrogen, sulfur, and selenium bridges changed the bond length alternation in the eight-membered core ring. The calculated results with (DFT B3LYP/6-31+G) correlate well with the experimental results obtained from X-ray crystallographic studies (Table S2, Supporting Information (SI)), with the exception of the maximum deviation of the bent angle α of **6** (26.7° vs 8.9°).

In the crystal structure of **3**, the molecule consists of a crystallographic 2-fold screw axis passing through the center of an eight-membered ring, including an inversion center (Figure 2). Adjacent molecules are found to be stacked in a concave–

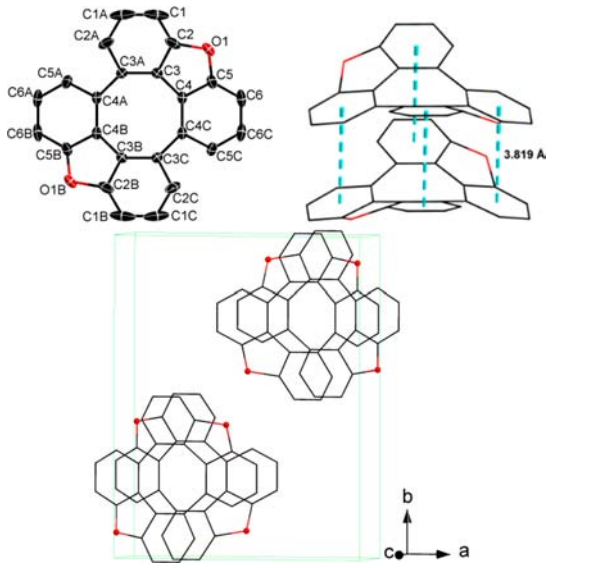

Figure 2. Crystal packing in the X-ray crystal structure of **3**.

Table 1. Selected Structural Data Analysis of Heteroatom-Bridged Tetraphenylenes[a]

X-ray	3	6	7	8	10
Bond length[Å]	1.48/1.43/	1.49/1.42/	1.49/1.41/	1.49/1.41/	1.50/1.40/
$r_1/r_2/r_3$	1.43	1.46	1.45	1.46	1.45
Bond angle[°]					
C1-C2-C3	127.03	128.18	126.85	126.79	127.22
C2-C3-C4	137.38	136.68	135.40	130.66	128.79
Torsion angle[°]					
C1-C2-C3-C4	9.53	12.45	9.80	11.97	15.54
C1-C2-C5-C6	40.46	38.80	47.55	57.94	62.59
Dihedral angle A/B[°]	7.64	5.43	9.41	14.82	12.66
Bent angle α[°]	25.56	8.89	28.84	35.32	37.43

[a]Determined by X-ray analysis.

dx.doi.org/10.1021/ol501267z | *Org. Lett.* 2014, 16, 3252–3255

convex manner with a $\pi-\pi$ distance of 3.82 Å as measured from the center of one benzene ring to the plane of the neighboring benzene ring. In comparison, the crystal structure of **8** exhibits an offset π-stacking with a distance of 3.52 Å between the edges of adjacent molecules as shown in Figure 3.

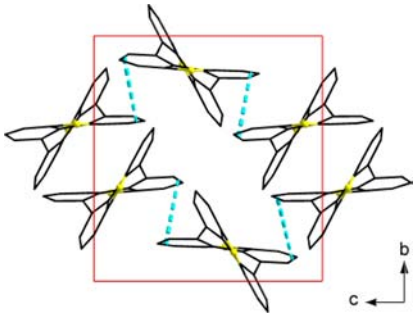

Figure 3. Packing observed in the X-ray crystal structure of **8**.

In the case of **6**, both the bend angle α and dihedral angle (A/B) values greatly decrease to 8.9° and 5.4° when compared with that of **7** (28.8° and 9.4°, respectively). The carbazole units and parent eight-membered ring are even much closer to planar, probably due to the presence of outstretched sterically hindered benzene rings. The crystal packing of **6** suggests the existence of an intermolecular $\pi-\pi$ stacking between the π systems of the closet molecules (Figures 4), and weak aromatic intermolecular $\pi-\pi$ stacking interaction between neighboring molecules was observed from the crystal packing of **7** (Figure S3, SI).

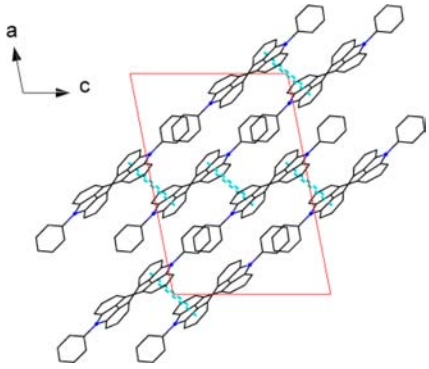

Figure 4. Packing observed in the X-ray crystal structure of **6**.

The optical properties of **3**, **5**, **8**, and **10** were investigated by both UV/vis and fluorescence spectroscopy. When compared with **1**, compounds **3**, **5**, **8**, and **10** exhibit a red shift λ_{max} (by ca. 1, 11, 24, and 26 nm, respectively). The absorptions of these heteroatom-bridged tetraphenylenes are similar; all of them show a strong intense absorption band with two shoulders. Moreover, a weak absorption band in the longer-wavelength region, ranging from 300 to 420 nm, is observed in **3**, **5**, **8**, and **10**. According to theoretical calculations, this long-wavelength absorption is mainly attributed to the HOMO−LUMO transition of **3**, **5**, **8**, and **10**, which suggests the existence of n$-\pi$ conjugation between the lone pair electrons on the oxygen, nitrogen, sulfur, and selenium atoms and the π-conjugated biphenylene framework (Figure 5). Compound **5** exhibits blue luminescence with an emission maximum from 410 to 550 nm, which is close to that of the parent carbazole

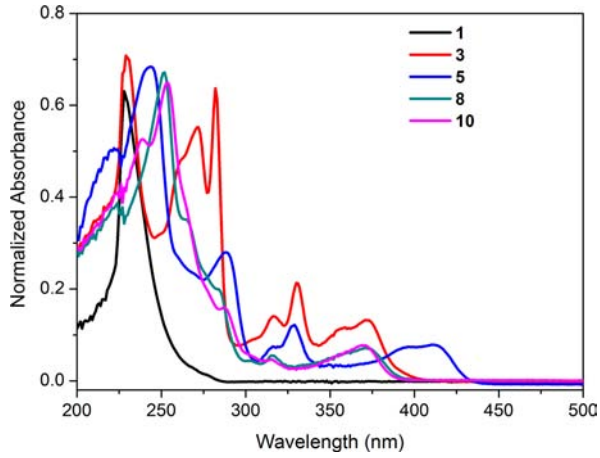

Figure 5. Normalized UV/vis absorption (CH_2Cl_2) of heteroatom-bridged tetraphenylenes.

unit. In contrast, **6** exhibits the strongest fluorescence among these heteroatom-bridged tetraphenylenes (Figure S10, SI).

A comparative analysis between the dibenzo analogues (benzofuran, carbazole, and benzothiophene) and these heteroatom-bridged tetraphenylenes (**3**, **5**, **8**, **10**) was also carried out. The α-protons of the dibenzo units in heteroatom-bridged tetraphenylenes (**3**, **5**, **8**, and **10**) show an upfield shift as compared with the corresponding protons in the relevant dibenzo compounds. These upfield shifts are principally ascribed to the change of paratropic ring current in the heteroatom-bridged tetraphenylenes. The longest absorption maximum λ_{max} (by ca. 1, 9, and 16 nm, respectively) of **3**, **5**, and **8** is bathochromically shifted compared with those of benzofuran, carbazole, and benzothiophene, which may suggest the existence of π-conjugation between the corresponding two dibenzo units in the heteroatom-bridged tetraphenylene framework (Table S1, SI).

As demonstrated in Figure S17 (SI), the electrochemical behavior of these heteroatom-bridged tetraphenylenes (**3**, **6**, **8**, **10**) was evaluated employing cyclic voltammetry and DFT methods. The cyclic voltammogram of **3** shows one irreversible oxidation wave with a peak potential at 1.21 V and two quasi-reversible reduction waves with half-wave reduction potentials at−2.32 V and−2.64 V versus ferrocenium/ferrocene. From these potentials, the HOMO energy level (E_{HOMO}) and LUMO energy level (E_{LUMO}) for **3** are estimated as−6.31 eV, −2.78 eV, respectively.[11] The values of E_{LUMO} and E_{HOMO} of **3** are almost the same as those of **8**, indicating both compounds have similar electrochemical properties. From the oxidation wave of **6**, the HOMO energy level of this compound is estimated as −5.78 eV, which, together with the molecular packing of **6** in crystals, suggests that **6** is a candidate for a p-type semiconductor.[12] Furthermore, the calculated HOMO and LUMO energy levels are in reasonable agreement with the experimental values determined by cyclic voltammetry (Table S3 and Figure S17, SI).

In conclusion, novel heteroatom-bridged tetraphenylenes (**3**, **5**, **6**, **7**, **8**, and **10**) were prepared from **2** or **4**, whose configurations were efficiently adjusted using different bridging atoms. Crystallographic investigations indicate that **3**, **6**, **7**, **8**, and **10** assume a unique saddle-shaped structure with different packing motifs. The HOMO energy level and $\pi-\pi$ stacking in the crystal structures suggest some of these heteroatom-bridged tetraphenylenes are potential candidates for electronic materi-

dx.doi.org/10.1021/ol501267z | Org. Lett. 2014, 16, 3252−3255

als. Further investigations of their semiconductor properties are in progress.

■ ASSOCIATED CONTENT

Supporting Information

Descriptions of experimental procedures for compounds and analytical characterization. This material is available free of charge via the Internet at http://pubs.acs.org.

■ AUTHOR INFORMATION

Corresponding Author

*E-mail: hncwong@cuhk.edu.hk.

Notes

The authors declare no competing financial interest.

■ ACKNOWLEDGMENTS

This work was supported by an Area of Excellence Scheme established under the Research Grants Council of the Hong Kong SAR, China (Project No. AoE/P-03/08) and a grant to the State Key Laboratory of Synthetic Chemistry from the Innovation and Technology Commission. Grants from the National Natural Science Foundation of China (NSFC No. 21272199), The Chinese Academy of Sciences−Croucher Foundation Funding Scheme for Joint Laboratories, the Shenzhen Science and Technology Innovation Committee for the Municipal Key Laboratory Scheme (ZDSY20130401150914965), and the Shenzhen Basic Research Program (JCYJ20120619151721025) are also gratefully acknowledged. We thank Professor Thomas C. W. Mak and Dr. Chun-Kit Hau (The Chinese University of Hong Kong) for helping to carry out X-ray crystallographic analyses.

■ REFERENCES

(1) (a) Rapson, W. S.; Shuttleworth, R. G.; Niekerk, J. N. *J. Chem. Soc.* **1943**, 326−327. (b) Irngartinger, H.; Reibel, W. R. K. *Acta Crystallogr.* **1981**, *37*, 1724−1728. (c) Mak, T. C. W.; Wong, H. N. C. *Top. Curr. Chem.* **1987**, *140*, 141−164.

(2) (a) Peng, H.-Y.; Lam, C. K.; Mak, T. C. W.; Cai, Z.; Ma, W.-T.; Li, Y.-X.; Wong, H. N. C. *J. Am. Chem. Soc.* **2005**, *127*, 9603−9611. (b) Huang, H.; Hau, C.-K.; Law, C. C. M.; Wong, H. N. C. *Org. Biomol. Chem.* **2009**, *7*, 1249−1257. (c) Hau, C.-K.; He, H.; Lee, A. W. M.; Chik, D. T. W.; Cai, Z.; Wong, H. N. C. *Tetrahedron.* **2010**, *66*, 9680−9874.

(3) (a) Wuckert, E.; Hägele, C.; Giesselmann, F.; Baro, A.; Laschat, S. *Beilstein J. Org. Chem.* **2009**, *5*, 57−64. (b) Hägele, C.; Wuckert, E.; Laschat, S.; Giesselmann, F. *ChemPhysChem* **2009**, *10*, 1291−1298. (c) Hau, C. K.; Chui, S. S. Y.; Lu, W.; Che, C. M.; Cheng, P. S.; Mark, T. C. M.; Miao, Q.; Wong, H. N. C. *Chem. Sci.* **2011**, *2*, 1068−1075.

(4) (a) Rathore, R.; Magueres, P. L.; Lindeman, S. V.; Kochi, J. K. *Angew. Chem., Int. Ed.* **2000**, *39*, 809−812. (b) Ogasawara, J.; Igarashi, T.; Sano, S. U.S. Pat. Appl. US 20050112407, 2005.

(5) Nielsen, C.; Brock-Nannestad, T.; Reenberg, T.; Hammershoj, P.; Christensen, J.; Stouwdam, J.; Pittelkow, M. *Chem.—Eur. J.* **2010**, *16*, 13030−13034.

(6) (a) Feng, C.; Kuo, M.; Wu, Y. *Angew. Chem., Int. Ed.* **2013**, *52*, 7791−7794. (b) Nielsen, C.; Brock-Nannestad, T.; Hammershoj, P.; Reenberg, T.; Schau-Magnussen, M.; Trpcevski, D.; Hensel, T.; Salcedo, R.; Baryshnukov, G.; Minaev, B.; Pittelkow, M. *Chem.—Eur. J.* **2013**, *19*, 3898−3904. (c) Miller, R.; Duancan, A.; Schneebeli, S.; Gray, D.; Whalley, A. *Chem.—Eur. J.* **2014**, *20*, 3705−3711. (d) Yuan, C.; Saito, S.; Camacho, C.; Kowalczyk, T.; Irle, S.; Yamaguchi, S. *Chem.—Eur. J.* **2014**, *20*, 2193−2200.

(7) (a) Erdtman, H.; Höberg, H. E. *Chem. Commun.* **1968**, 773−774. (b) Ohmae, T.; Nishinaga, T.; Wu, M.; Iyoda, M. *J. Am. Chem. Soc.* **2010**, *132*, 1066−1074. (c) Brock-Nannestad, T.; Nielsen, C. B.; Schau-Magnussen, M.; Hammershoj, P.; Reenberg, T.; Petersen, A.; Trpcevski, D.; Pittelkow, M. *Eur. J. Org. Chem.* **2011**, 6320−6325. (d) Hensel, T.; Trpcevski, D.; Lind, C.; Grosjean, R.; Hammershoj, P.; Nielsen, C.; Brock-Nannestad, T.; Nielsen, B.; Schau-Magnussen, M.; Minaev, B.; Baryshnukov, G.; Pittelkow, M. *Chem.—Eur. J.* **2013**, *19*, 17097−17102.

(8) Lin, F.; Peng, H. Y.; Chen, J. X.; Chik, D. T. W.; Cai, Z.; Wong, K. M. C.; Yam, V. W. W.; Wong, H. N. C. *J. Am. Chem. Soc.* **2010**, *132*, 16383−16392.

(9) Kabir, S. M. H.; Iyoda, M. *Synthesis* **2000**, 1839−1843.

(10) The relevant iodide intermediate in Scheme 3 was identified as 1,8-dibromo-9,16-diiodotetraphenylene after treatment of compound **4** with *n*-BuLi and I_2.

(11) The commonly used formal potential of the ferrocenium/ferrocene redox couple in the Fermi scale is −5.1 eV, which is calculated on the basis of an approximation neglecting solvent effects using a work function of 4.46 eV for the normal hydrogen electrode (NHE) and an electrochemical potential of 0.64 V for ferrocenium/ferrocene versus NHE. See: Cardona, C. M.; Li, W.; Kaifer, A. E.; Stockdale, D.; Bazan, G. C. *Adv. Mater.* **2011**, *23*, 2367−2371.

(12) Tang, M. L.; Reichardt, A. D.; Wei, P.; Bao, Z. *J. Am. Chem. Soc.* **2009**, *131*, 5264−5273.